[CANCER RESEARCH 54, 4791–4797, September 1, 1994]

Overexpression of Metalloproteinase Inhibitor in B16F10 Cells Does Not Affect Extravasation but Reduces Tumor Growth[1]

Sahadia Koop, Rama Khokha, Eric E. Schmidt, Ian C. MacDonald, Vincent L. Morris, Ann F. Chambers, and Alan C. Groom[2]

Departments of Medical Biophysics [S. K., E. E. S., I. C. M., A. F. C., A. C. G.], Oncology [R. K., V. L. M., A. F. C.], Biochemistry [R. K.], Microbiology and Immunology [V. L. M., A. F. C.], University of Western Ontario; London Regional Cancer Centre [R. K., A. F. C.]; and John P. Robarts Research Institute [A. C. G.], London, Ontario N6A 5C1, Canada

ABSTRACT

It is widely accepted that a major role of matrix metalloproteinases in the metastatic process is degradation of basement membrane during cancer cell invasion. We tested the hypothesis that the reduction in metastatic potential which has been demonstrated for B16F10 melanoma cells genetically engineered to overexpress tissue inhibitor of metalloproteinase-1 (TIMP-1) is caused by a decrease in their ability to extravasate. Using intravital videomicroscopy of chick embryo chorioallantoic membrane, we studied extravasation of B16F10 cells and B16F10 cells transfected to overexpress TIMP-1. More than 800 cells in 36 chick embryos were analyzed for each cell line during 72 h postinjection. TIMP-1 up-regulation had no effect on the time course of extravasation, virtually all cells from both cell lines having extravasated by 36 h. We also studied the morphology of micrometastases at days 3 and 7. Lack of contact between cancer cells within micrometastases at day 3 and reduction in size and number of tumors at day 7 were observed for TIMP-1 overexpressor cells compared to B16F10. Our findings illustrate that the imbalance between TIMP and metalloproteinases created by overexpression of TIMP-1 in B16F10 cells reduces their metastatic ability *in vivo* by affecting tumor growth postextravasation.

INTRODUCTION

Metastasis, or secondary neoplastic growth, defines malignancy and is a major contributor to cancer mortality. A better understanding of the molecular mechanisms involved in this process could lead to new strategies for more effective therapies against metastasis. The metastatic process has been proposed to consist of several sequential events including escape of cancer cells from the original tumor, intravasation and dissemination through blood and lymphatic vessels, arrest in the microvasculature of target organs, extravasation, and growth at a new site (1–4). Since basement membrane and extracellular matrix provide the main physical barriers to cancer cell invasion, proteolytic degradation of these structures has been proposed to be important in the metastatic process (5, 6).

MMPs[3] are members of a family of Zn^{2+}-dependent endopeptidases with a broad spectrum of proteolytic activity for the basement membrane and several components of the extracellular matrix (7). The MMP family includes collagenases, gelatinases, and stromelysins (8). The activity of MMPs is regulated by two mechanisms: (*a*) the secretion of these enzymes in an inactive proenzyme form, requiring activation; and (*b*) the formation of an irreversible 1:1 stoichiometric complex between TIMP and the activated or latent enzyme (9). Three distinct vertebrate TIMPs have been characterized thus far: TIMP-1 (10), TIMP-2 (11), and TIMP-3 (12). The activity of all MMPs is effectively inhibited by any member of the TIMP family (13). The balance between MMPs and TIMPs is an important factor in determining invasion and metastasis by cancer cells (6, 14, 15).

An inverse correlation between TIMP-1 levels and metastatic ability has been reported in a series of fibrosarcomas (16), and addition of exogenous TIMP-1 to B16BL6 melanoma cells has been shown to decrease their invasive ability in amnion invasion chambers (17). Down-regulation of TIMP-1 expression by transfection of antisense TIMP DNA into mouse Swiss 3T3 cells enhanced their ability to invade human amniotic membranes *in vitro* and to form metastatic tumors in athymic mice (18). Murine B16F10 melanoma cells transfected to overproduce TIMP-1 showed a significant reduction in their invasive ability in a Matrigel transwell invasion assay (19) and an inhibition of experimental metastatic ability *in vivo* in chick embryo and mouse (20, 21). Up-regulation of TIMP-2 achieved by transfection of invasive and metastatic rat embryo cells produced partial suppression of lung colony formation after i.v. injection and completely inhibited local tissue invasion after s.c. injection in nude mice (22).

The present study analyzed and compared the metastatic process of B16F10 cells *versus* the genetically engineered TIMP-1 overexpressor B16F10 cells in chick embryo CAM, the respiratory organ of the embryo. High-resolution intravital videomicroscopy was used, a technique that we recently developed to study the metastatic process in chick embryo (23, 24) and mouse (25) models. Successive steps in the metastatic process can be observed as they occur *in vivo*. In this study, the positions and interactions of cancer cells were directly monitored and recorded at various times from immediately after injection until 7 days later.

Our hypothesis was that the reduction in metastatic capacity of TIMP overexpressing B16F10 cells was caused by a decreased ability to extravasate. To our surprise, no difference was found in the timing of extravasation between the cell lines. However, we found that tumor growth, which occurred only after extravasation, was markedly suppressed in TIMP-1 overexpressor cells. Furthermore, the morphology of micrometastases resulting from TIMP-1 overexpressor cells was altered, showing reduction of contact between cancer cells with consequent dispersed distribution of the cells in the early stages of tumor formation.

Our results show that the imbalance between MMPs and TIMPs resulting from the overexpression of TIMP-1 in B16F10 cells decreases the metastatic ability of these cancer cells *in vivo*, not by reducing extravasation but by affecting tumor growth after extravasation.

MATERIALS AND METHODS

Cell Culture and Fluorescent Labeling. Cell lines used were B16F10 melanoma cells (26) and the transfected clone 6–5, produced by transfecting B16F10 cells with a TIMP-1 expression vector as described by Khokha *et al.*

Received 3/28/94; accepted 6/22/94.

The costs of publication of this article were defrayed in part by the payment of page charges. This article must therefore be hereby marked *advertisement* in accordance with 18 U.S.C. Section 1734 solely to indicate this fact.

[1] This work was supported in part by grants from the National Cancer Institute of Canada and the Cancer Research Society, Inc. S. K. is supported by a Brazilian Scholarship from CAPES (Fundação Coordenação de Aperfeiçoamento de Pessoal de Nível Superior). R. K. is a Medical Research Council of Canada Scholar, and A. F. C. is a Career Scientist of the Ontario Cancer Treatment and Research Foundation.

[2] To whom requests for reprints should be addressed.

[3] The abbreviations used are: MMP, matrix metalloproteinase; TIMP, tissue inhibitors of metalloproteinases; CAM, chorioallantoic membrane; p.i., postinjection; H&E, hematoxylin and eosin.

(19). *In vitro* TIMP-1 mRNA and protein levels are very low in B16F10 cells and 5- to 7-fold higher in clone 6–5 (19).

Cells were maintained in α-Minimum Essential Medium plus ribonucleosides (GIBCO/BRL, Burlington, Ontario, Canada) supplemented with 10% fetal calf serum (GIBCO/BRL). For the TIMP-1 overexpressor cells, G418 sulfate (GIBCO/BRL) at a final concentration of 400 μg/ml (active) was added to the medium. The number of cell passages was limited to eight; the cells were subcultured twice a week with 1% trypsin (GIBCO/BRL) in citrate saline solution (0.015 M trisodium citrate-0.13 M potassium chloride, pH 7.4). The level of TIMP expression of the TIMP-1 overexpressor cells was confirmed by mRNA analysis immediately before cell labeling. Cells from subconfluent monolayers were fluorescently labeled with Calcein-AM (Molecular Probes, Inc., Eugene, OR; Ref. 25) and kept on ice before injection.

To determine the *in vitro* plating efficiency, labeled or unlabeled (control) cells were plated in 60-mm tissue culture dishes at 100 cells/dish ($n = 6$) and kept undisturbed in the incubator. After 11 days, colonies were counted, and plating efficiencies were calculated (number of colonies/total number of cells plated). The relative plating efficiency of labeled cells was 95% that of unlabeled controls for B16F10 cells and 96% that of unlabeled controls for the TIMP-1 overexpressor cells.

Membrane integrity of the labeled cancer cells was assessed before the experiments by adding a drop of ethidium bromide (0.01 mg/ml) to an equal volume of cells on a coverslip. Cells were scored by fluorescence microscopy as either excluding ethidium bromide (green fluorescence) or as having taken it up (red fluorescence) as described (25). For both cell lines, 97% of the cells excluded ethidium bromide immediately before injection.

Experimental Metastasis Assay. Parental B16F10 and TIMP-1 overexpressor cells, fluorescently labeled, were injected (3×10^5 cells/embryo in 0.1 ml) i.v. into the CAM of 11- to 12-day chick embryos as described by Chambers *et al.* (24, 27). The mean cell diameter before injection was 19.3 μm ± 6.7 (SD; $n = 50$; range, 13.1–42.1 μm) for control B16F10 cells and 17.4 μm ± 3.9 (SD; $n = 50$; range, 13.3–21.0 μm) for TIMP-1 overexpressor cells. B16F10 cells are highly metastatic in the CAM of chick embryos, but metastases are also seen in a variety of internal organs such as liver, heart, and lung (20, 27). Overexpression of TIMP-1 in B16F10 cells reduces the metastatic ability of these cells in chick embryo (20). The interactions of these two cell lines with the microcirculation of the CAM were studied by intravital videomicroscopy (see below). The embryos were analyzed at regular time intervals p.i. from immediately following injection up to 7 days to determine the percentage of cells at intra- and extravascular locations and also to study the morphology of micrometastases. Each embryo was observed for approximately 2–4 h; the time intervals analyzed were: every 2 h up to day 1, 12 h up to day 2, and 24 h up to day 7.

Fluorescence was used to identify all injected cells up to ~24 h p.i. because at the time of injection very few cells contained detectable amounts of melanin. Criteria for identification of cancer cells after 24 h p.i. (when the fluorescence had disappeared) were the presence of melanin, which increased with time, and the cell diameter, which is markedly greater than for WBC and other cells of the CAM. To rule out any difference in cell behavior related to the fluorescent labeling, we did two experiments for each cell line using non-labeled cells. No differences were found between results from labeled and non-labeled cells. In addition, three embryos were primed with ethidium bromide solution (0.01 mg in 0.1 ml), injected i.v. immediately before the injection of cancer cells to permit *in vivo* assessment of the membrane integrity of cells after injection as described previously (25). Cell membrane disruption is indicated by the uptake of ethidium bromide, resulting in red fluorescence.

Intravital Microscopy and Analysis of Data. The procedure for intravital microscopy of chick embryo CAM has been described in detail previously (23, 24). Briefly, eggs were removed from the incubator at specific times after injection of cancer cells, and the shell and outer shell membrane over the air sac were removed. The outer and inner shell membranes were separated further on one side, and a small portion of shell was removed to provide a window for oblique illumination. Paraffin oil was applied to the exposed inner shell membrane to render it transparent and reveal the CAM vessels. For observation of cancer cells immediately following injection, one of these veins was used for injection rather than one exposed by a window in the side of the egg. The egg was placed on an acrylic platform on the stage of an inverted microscope (Nikon, Diaphot TMD) with the exposed membrane downward on a coverslip window, positioned above the objective lenses (×10 to 100). The tissue was transilluminated obliquely with a fiber optic light guide. For identification of injected cancer cells, episcopic illumination with the fluorescence excitation wavelength (450–490 nm) was also used. Images were viewed using a black and white video camera (Panasonic WV 1550; Newvicon) and monitor. A character generator added time, date, and stopwatch information, and the combined signal was recorded on SVHS video tapes.

Intravital microscopy of the CAM allows clear observation of the extensive capillary plexus which is served by arterioles and venules in the underlying mesenchyme layer. Blood arrives at the plexus via arterioles and leaves it, oxygenated, via venules. Orifices connect the capillary plexus to small arterioles and venules. Cancer cells could be identified by fluorescence, except that gradual loss of the Calcein-AM fluorescence during the experiments resulted from the limited "half-life" of this dye intracellularly and quenching from repeated brief exposures to the fluorescence excitation illumination. Cells in transit from the microvasculature to the underlying mesenchymal tissue were identified by focusing alternately on the plexus level and the mesenchyme using higher magnifications (×60 and 100 objectives). The visual appearance of the extravasation process was a gradual "sinking" of the cell out of the plane of the capillary plexus, allowing red blood cell flow to occur over the top of the extravasating cell. Stop-frame images were digitized and enhanced by computer software (Optimas; BioScan) to clearly define vessel walls and cancer cells. This software allowed us to make measurements of diameters and areas of cells and tumors as well as distances between the visualized structures. Photographs of video images were made directly from the monitor using a 35 mm camera.

For statistical analysis, means and medians of the percentage of cells at specific locations were determined for each time interval, based on the number of experiments. Mann-Whitney U tests were used to compare results for the two cell lines because several of the populations analyzed did not show a normal distribution (28). A level of $P < 0.05$ was regarded as statistically significant.

Histology and Cell Morphometry. To confirm the findings from intravital videomicroscopy and to identify tissue components present within micrometastases, we prepared histological sections from CAMs at 3 days and 7 days p.i. For each cell line, three CAMs were used at both time points, and 3–4 sections/CAM were stained by H&E or the Feulgen technique. The characterization of amelanotic cells as cancer cells after 24 h p.i. when little fluorescence was detectable was confirmed by Feulgen staining, which showed the nuclear ploidy of individual cells. H&E staining was used to study individual micrometastases and to characterize their size, number, and melanin content. Statistical evaluation of the results was carried out as described above.

RESULTS

After i.v. injection of fluorescently labeled B16F10 or TIMP-1 overexpressor cells into the CAM, we analyzed their positions at various times and determined the growth of micrometastases. To study events up to and including extravasation, a total of 818 B16F10 cells and 870 TIMP-1 overexpressor cells were identified and individually analyzed by intravital videomicroscopy during the first 72 h p.i. To study morphology and growth of micrometastases from days 3 to 7, both intravital videomicroscopy and histology were used.

Events Prior to Extravasation. B16F10 and TIMP-1 overexpressor cells showed no difference in their behavior during events prior to extravasation from the capillary bed to the underlying mesenchyme. By 1 min p.i., all observed cells were found arrested inside the CAM microcirculation, apparently by size restriction. Cell membrane integrity was preserved over a period of at least 3 h p.i. as assessed from ethidium bromide exclusion by 99% of cells from both cell lines. Pinching off of membrane enclosed fragments (clasmatosis, 25) occurred in some cells after their arrest in the microvasculature, but no difference in the timing or extent of this process was detected between the two cell lines (data not shown). These findings do not differ from those which we reported for B16F10 cells in mouse liver (25). Fig. 1 shows photographs of representative cancer cells and their interactions with the microvasculature, before and after extravasation.

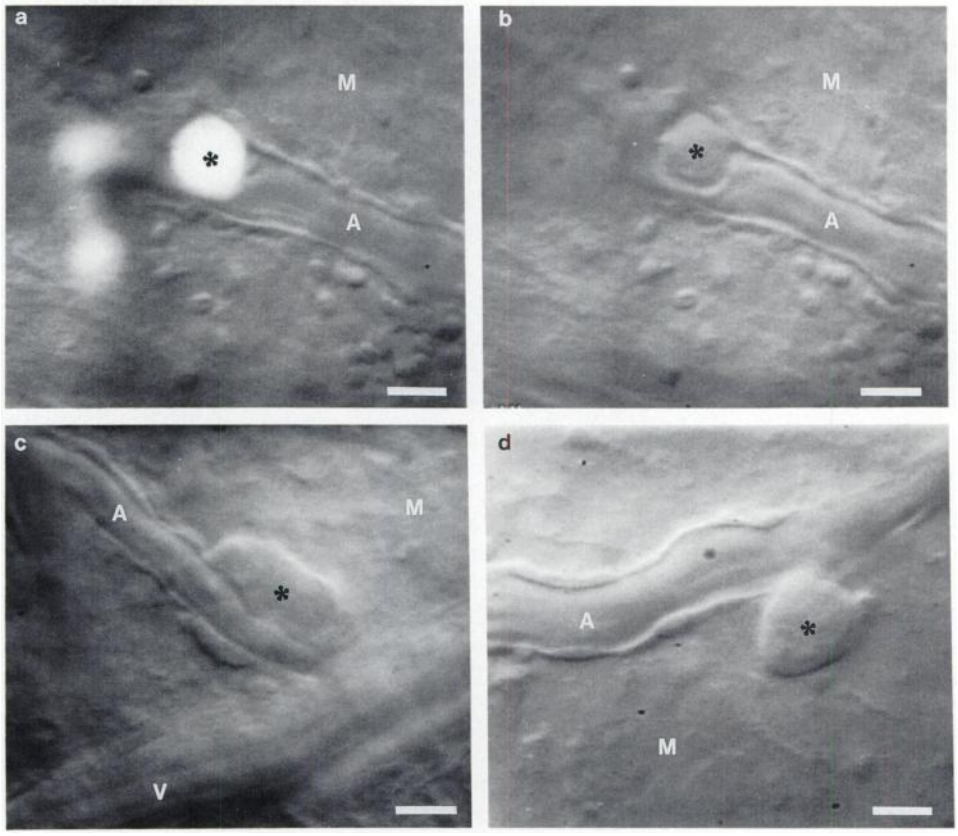

Fig. 1. Representative photographs of intravascular or extravasated B16F10 melanoma cells viewed by intravital videomicroscopy. *a*, a TIMP-1 overexpressor cell (*) labeled with Calcein-AM arrested in the arteriolar lumen (*A*) observed with transillumination in combination with epifluorescence at 9 min p.i. Two additional labeled cells outside of the plane of focus are also evident. *b*, the same cell (*) observed with transillumination alone. *c*, an extravasated B16F10 cell (*) wrapping around a terminal arteriole (*A*) at 40 h p.i. *V*, a venule lying slightly below the plane of focus. *d*, an extravasated TIMP-1 overexpressor cell (*) in contact with a terminal arteriole (*A*) at 28 h p.i. *M*, mesenchyme tissue. Bars (*a-d*), 20 μm.

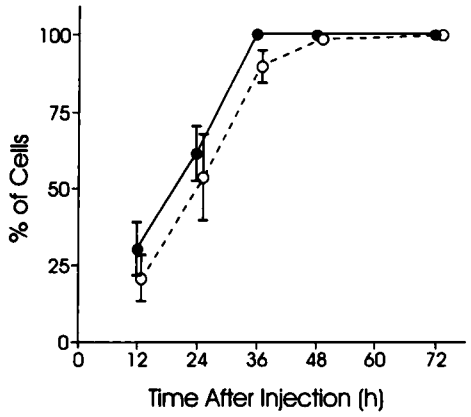

Fig. 2. Time course of extravasation of parental B16F10 (●) and TIMP-1 overexpressor (○) cells. Percentage of cells in the CAM that were extravasated was plotted as a function of time after injection. *Points*, cumulative values (means; n = 3–16) from the previous time point to the time indicated, based on the number of experiments. A total of 36 embryos was used for each cell line. *Bars*, SE.

Within the first 15 min p.i., very few cells were melanotic, 5.0% of B16F10 cells and 1.5% of TIMP-1 overexpressor cells.

Kinetics of Extravasation. No significant difference in the ability to extravasate was found between B16F10 and TIMP-1 overexpressor cells. The time course of extravasation for both cell lines is shown in Fig. 2. All B16F10 cells were intravascular until 4 h p.i., at which point some cells started to extravasate, whereas a few TIMP-1 overexpressor cells started as early as 2 h p.i. By 36 h p.i., 100% of B16F10 cells and 89.9% of TIMP-1 overexpressor cells had extravasated. No statistically significant difference was found in the percentage of extravasated B16F10 or TIMP-1 overexpressor cells by analyzing median values at given times from 0–72 h p.i.

During the process of extravasation, cells from both lines changed their shapes, showing cell extensions which protruded in the direction of the underlying mesenchyme. After extravasation, these cells reacquired their rounded shape (Fig. 1*d*) or presented cell extensions wrapping around microvessels (Fig. 1*c*). No visible damage to the vessel wall was evident during or after extravasation. The sizes of cells that extravasated *in vivo* covered the entire size range measured *in vitro*. In both cell lines, a lateral movement of extravasated cancer cells toward vascular sites (mainly arterioles) within the mesenchyme was observed (data not shown) as we reported for B16F1 cells (24).

Postextravasation Growth of Micrometastases. The timing of first cell division was monitored from 0–72 h p.i., and no statistically significant difference was found between B16F10 and TIMP-1 overexpressor cells (Fig. 3). First cell division was identified by the

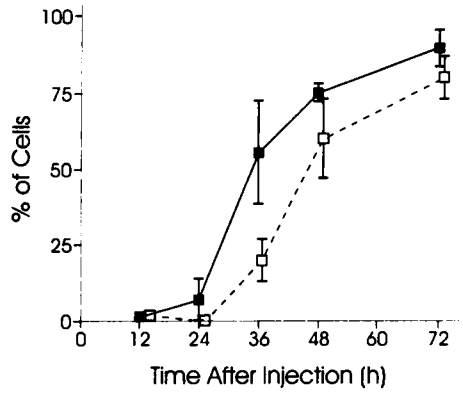

Fig. 3. Timing of initial division of parental B16F10 (■) and TIMP-1 overexpressor (□) cells. Percentage of cells that had divided was plotted as a function of time after injection. *Points*, cumulative values (means; n = 3–16) from the previous time point to the time indicated, based on the number of experiments. A total of 36 embryos was used for each cell line. *Bars*, SE.

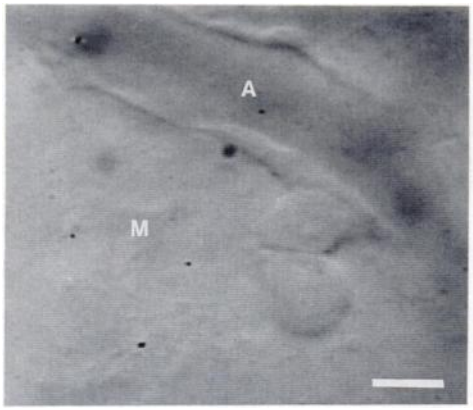

Fig. 4. First division of an amelanotic TIMP-1 overexpressor B16F10 cell at 28 h p.i. The cells are close to an arteriole (*A*). *M*, mesenchyme tissue. *Bar*, 20 μm.

presence of two cohesive cancer cells, having a large flattened interface between them (Fig. 4). In contrast, pairs of cells that maintained a round shape with only a very limited area of contact were considered as being separate cells that had extravasated together (this was observed only rarely). Evidence of cell division was first seen at 12 h p.i., and by 72 h p.i., more than 80% of the cells from both cell lines had divided. Cancer cell division was seen only after extravasation during intravital microscopic studies of both cell lines. This finding was confirmed by histological analyses of tissue sections, which showed no cancer cell inside vessels at days 3 and 5.

Tumor morphology was clearly different between B16F10 and TIMP-1 overexpressor cells at days 2 to 4. Micrometastases from TIMP-1 overexpressor cells predominantly contained amelanotic cells, which presented an unusual lack of homotypic cell contact. In marked contrast, tumors formed by B16F10 cells were very compact. Photographs from intravital videomicroscopy (Fig. 5, *a* and *b*) and histological tissue sections (Fig. 6, *a* and *b*) show the difference in cell contact between B16F10 and TIMP-1 overexpressor cells at day 3. The mean distance between cells within the same micrometastasis at this time was 3.7 μm ± 0.7 (SD; $n = 10$) for TIMP-1 overexpressor cells, compared to only 0.3 μm ± 0.2 (SD; $n = 10$) for B16F10 cells. Extracellular matrix and a few stromal cells could be seen between amelanotic TIMP-1 overexpressor cells in histological sections (Fig. 6*b*). At day 3, CAMs injected with TIMP-1 overexpressor B16F10 cells showed a larger area per tumor compared with the tumors from B16F10 parental cells (Table 1). This was due to the sparse distribution of TIMP-1 overexpressor cells within individual tumors, contrasting with the compact distribution exhibited by B16F10 cells. The mean number of cells per tumor at day 3 is shown in Table 1. CAMs injected with TIMP-1 overexpressor cells also showed more tumors/unit area at day 3 compared with CAMs from B16F10 cells (Table 1). In addition, 50% of the tissue sections of CAMs injected with TIMP-1 overexpressor cells showed melanin dispersed outside the tumors, whereas those injected with B16F10 cells did not show this.

By day 6, CAMs injected with B16F10 cells showed more tumors/unit area as well as a larger area/tumor than CAMs injected with TIMP-1 overexpressor cells (Table 1, day 7), and tumors from both cell lines displayed close cell-to-cell contact (Fig. 5, *c* and *d*; Fig. 6, *c* and *d*). All tumors surrounded arterioles and venules. Tumors from B16F10 cells were more melanotic at day 7 than those from TIMP-1 overexpressor cells (Table 1). Photographs from intravital videomicroscopy (Fig. 5, *c* and *d*) and from tissue sections (Fig. 6, *c* and *d*) show tumors from both cell lines at days 6 to 7.

DISCUSSION

Degradation of basement membrane is considered to be a major contribution of metalloproteinases to the metastatic process (15, 22). We tested the hypothesis that the reduction in metastatic potential that has been demonstrated for B16F10 melanoma cells genetically engineered to overexpress TIMP-1 is caused by a decrease in their ability to extravasate as a consequence of the inhibition of matrix metallo-

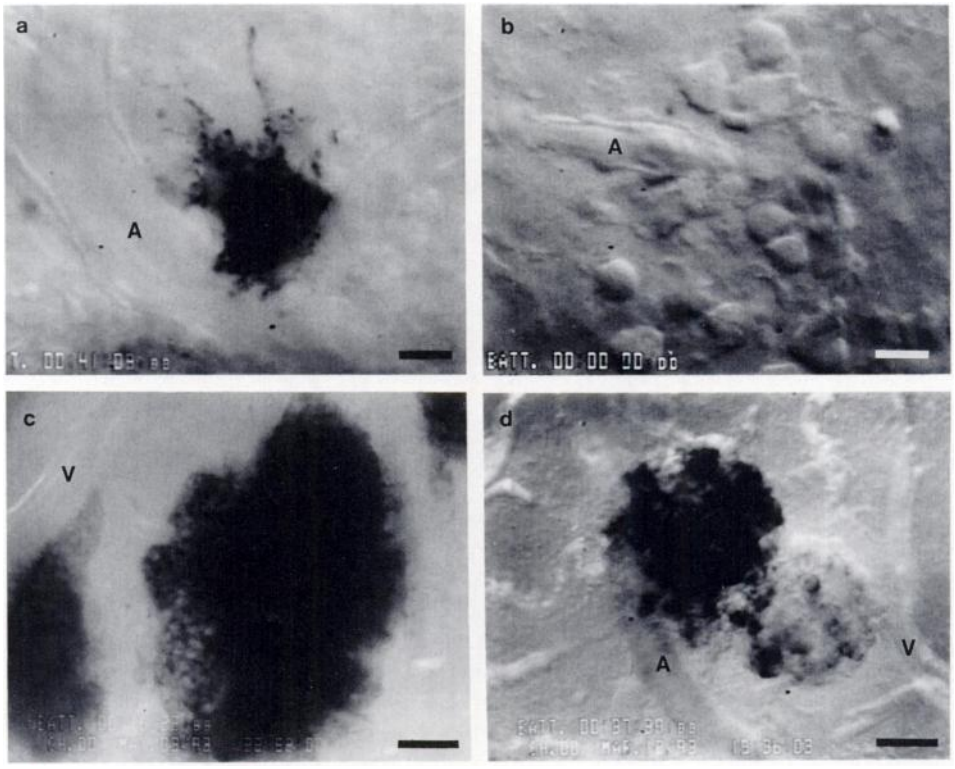

Fig. 5. Photographs from intravital videomicroscopy. *a*, a compact and melanotic tumor from parental B16F10 cells at 3 days p.i. The small tumor is wrapping around a bifurcation of an arteriole (*A*). *b*, a tumor from TIMP-1 overexpressor cells at 3 days p.i. showing dispersed and amelanotic cells around an arteriole (*A*). *c*, large melanotic tumors from parental B16F10 cells at 7 days p.i. At this stage, all the tumors are in contact with arterioles and venules (*V*). *d*, one mostly melanotic and one mostly amelanotic tumor from TIMP-1 overexpressor cells at 7 days p.i. Both tumors are in contact with arterioles (*A*) and venules (*V*). *Bars: a* and *b*, 20 μm; *c* and *d*, 100 μm.

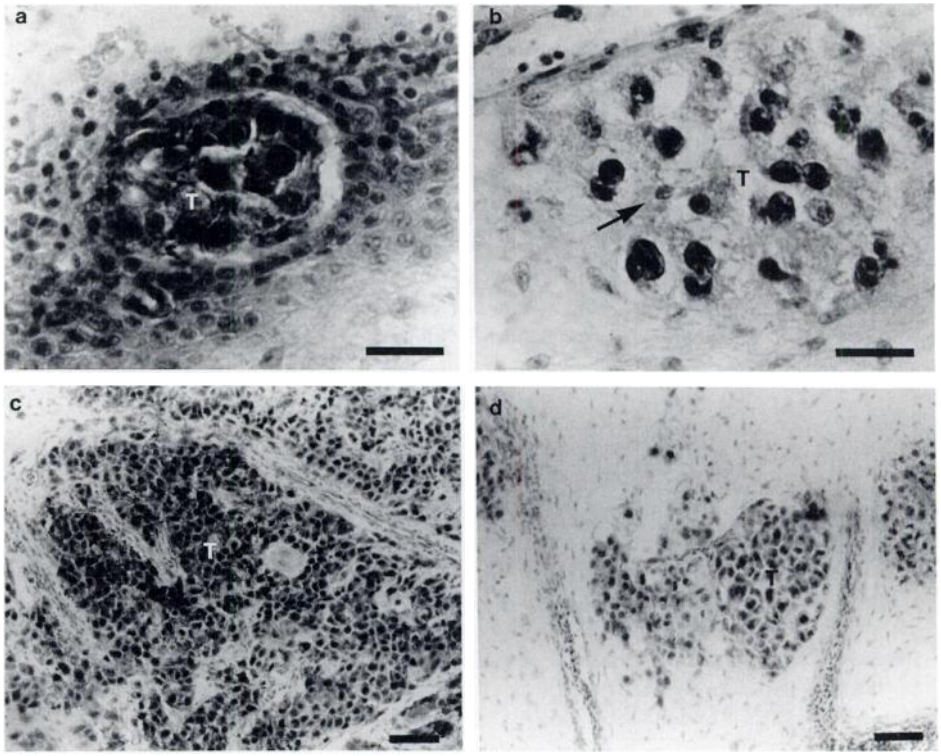

Fig. 6. Photographs from histological sections stained with H&E. *a*, a melanotic tumor from parental B16F10 cells at 3 days p.i. showing the typical close cell contact. *b*, a typical tumor from TIMP-1 overexpressor cells at 3 days p.i. showing poorly cohesive cancer cells with the presence of stromal cells and a large amount of extracellular matrix between them. *Arrow*, a stromal cell. *c*, large melanotic tumors from parental B16F10 cells at 7 days p.i. in close contact to each other. *d*, small and compact tumors from TIMP-1 overexpressor cells at 7 days p.i. *T*, tumors. *Bars: a* and *b*, = 20 μm; *c* and *d*, 50 μm.

proteinases. Using intravital videomicroscopy, we measured the time course of extravasation of parental B16F10 and TIMP-1 overexpressor cells from capillaries of the chorioallantoic membrane of 11–12-day old chick embryos. At this time, the basement membrane surrounding capillaries of the CAM is complete (29–31).

Surprisingly, overexpression of TIMP-1 in B16F10 cells had no effect on the time course of extravasation *in vivo*. However, it resulted in smaller and somewhat fewer metastases at day 7. A more dramatic difference between the two cell lines in terms of size and number of tumors at day 7 was reported by Khokha *et al.* (20), probably due to methodological differences. In that study, the CAMs were observed at low magnification with a dissecting microscope with the analysis being restricted to melanotic tumors above a certain size threshold. In contrast, the present study analyzed both melanotic and amelanotic tumors however small, and differences in tumor morphology between the two cell lines were detected as early as days 2 to 4. Our findings suggest that the imbalance of TIMP-1/MMP created by overexpression of TIMP-1 in B16F10 cells reduces their metastatic ability *in vivo* by affecting tumor growth postextravasation.

Some recent studies have suggested that inhibitors of metalloproteinases can affect tumor growth (20–22, 32); however, such evidence was based on analysis of tumor size at a relatively late stage of tumor development. Our approach allowed us to observe the metastatic process *in vivo*, starting from the time of injection to day 7, with analysis carried out at frequent time intervals. Therefore, we were able to observe the effect of TIMP-1 overexpression on individual early events in metastasis, such as extravasation and first cell division, as well as subsequent tumor growth. This is the first report to analyze extravasation in real time and demonstrate that TIMP-1 overexpression in B16F10 cells does not suppress their ability to extravasate *in vivo*. Our study suggests that regulation of proteolysis can contribute to the metastatic spread of tumors via a mechanism(s) which occurs after extravasation.

Lack of Effect of TIMP-1 on Extravasation. Contrary to our expectation, we found no difference in the time course of extravasation between B16F10 and TIMP-1 overexpressor cells. Previously, a significant reduction in the ability of the same TIMP-1 overexpressor cells to invade reconstituted basement membrane (Matrigel) had been reported (19). Extravasation through basement membrane *in vivo* thus seems to involve either different mechanisms or different amounts of metalloproteinases compared to the *in vitro* situation.

There are several possible explanations for the lack of effect of TIMP-1 on extravasation: (*a*) while a major constituent of basement membranes is type IV collagen, other components are also present. Proteases other than metalloproteinases (*e.g.*, serine and cysteine proteases) can also contribute to extravasation; (*b*) tumor cells can induce protease production by the adjacent normal tissue (33). Endothelial cells have been shown to produce increased latent collagenase and urokinase plasminogen activator activities in response to tumor promoters (34). Therefore, production of metalloproteinases by host tissue in our system could possibly be initiated equally well by TIMP-1 overexpressor and B16F10 cells; and (*c*) by increasing TIMP-1 expression, we may not have reduced the metalloproteinase

Table 1 *Morphometric measurements from histological tissue sections of parental B16F10 and TIMP-1 overexpressor B16F10 cells*

	Days p.i.	Parental		TIMP-1	
		Mean ± SE[a]	Median	Mean ± SE[a]	Median
No. of tumors/mm^2	3	2.3 ± 0.4	2.3	4.6 ± 0.9	3.7[b]
	7	7.0 ± 0.4	7.0	5.5 ± 0.9	4.4[b]
Area/tumor (μm^2)	3	1,150 ± 156	1,055	4,935 ± 525	5,134[b]
	7	75,109 ± 5,933	68,515	31,734 ± 7,410	30,390[b]
No. of cells/tumor[c]	3	10.9 ± 0.8	10.8	7.0 ± 0.5	7.3[b]
% of melanotic cells	3	80 ± 0.1	82	31 ± 0.1	29[b]
	7	96 ± 1.3	98	38 ± 0.1	36[b]

[a] n = 10, based on the number of sections.
[b] Significant difference ($P < 0.05$) from parental cell line (Mann-Whitney U test).
[c] It was not possible to determine this at day 7 due to the complex tumor morphology that had developed.

activity below a threshold required for extravasation to occur. The fact that no evidence of damage to vessel walls was seen during or after extravasation suggests that very low levels of protease activity may be sufficient for this process. In support of this hypothesis, electron microscopic studies with B16 melanoma and rat W/Fu AML cells showed that these cells intravasated capillaries by direct penetration through individual endothelial cells by means of transient migration pores, without destruction of the endothelial wall (35).

Our study confirms the intriguing finding of Chambers *et al.* (24) that after extravasation from the capillary plexus of the CAM, individual cancer cells migrate to the vicinity of arterioles and venules in the mesenchyme. There they grow as "collars" around preexisting vessels, forming metastases. This migration of cancer cells may represent a specific chemotactic response towards components of the extracellular matrix such as laminin and type IV collagen, which are known to be present in the vicinity of blood vessels of the CAM (29). Our study detected no differences in the ability of B16F10 and TIMP-1 overexpressor cells to undergo this lateral movement towards blood vessels. It is well known that, during metastasis, blood vessels grow into the developing tumors (36). TIMPs are capable of inhibiting this process (37–39). We did not observe angiogenesis in the thin tumors that developed in the CAM within 7 days of injection.

Effects of TIMP-1 on Tumor Growth. Overexpression of TIMP-1 in B16F10 cells decreased their metastatic activity by affecting processes that occur after extravasation at the level of tumor growth, although the timing of first cell division was not delayed. (No cancer cell division was observed inside vessels, using intravital videomicroscopy, as we reported before (24). Careful analysis of tissue sections showed no cancer cells or tumors inside vessels at days 3 and 7, confirming this finding.) Micrometastases formed by TIMP-1 overexpressor cells showed reduced homotypic contact after day 2, with stromal cells and a larger amount of extracellular matrix being detected in-between cancer cells. Another study (40) has shown that a high packing density of cells within tumors tends to be characteristic of more metastatic cell lines, in contrast to the low packing density found with more benign populations. It is intriguing that, although at day 3 the TIMP-1 overexpressor cells showed a lower packing density than B16F10 cells, by day 7, all tumors exhibited a closely packed arrangement of cells, and TIMP-1 overexpressor cells formed smaller and somewhat fewer metastases than the parental cell line.

The higher proportion of amelanotic cells in micrometastases from TIMP-1 overexpressor cells *versus* parental cells at days 3 and 7 p.i. raises the question whether the amelanotic cells grow more slowly and are responsible for the growth inhibition effect. This argument does not explain our findings because: (*a*) at the time of injection, ≥95% of cells from both cell lines were amelanotic, showing that there was no selection of an amelanotic subpopulation of TIMP-1 overexpressor cells. (The melanin content rose with time after injection for both cell lines.); (*b*) at 3 days p.i., micrometastases from both cell lines contained some amelanotic cells, but only the amelanotic TIMP-1 cells showed a lack of homotypic cell contact; and (*c*) at 7 days p.i., even the amelanotic TIMP-1 overexpressor cells within micrometastases showed very close cell contact. Therefore, these observations indicate that the slower growth rate of TIMP-1 overexpressor cells is not simply related to melanin content.

Other studies also have found evidence of a relationship between metalloproteinases and tumor growth. Up-regulation of TIMP-1 expression in B16F10 melanoma cells suppressed their metastatic ability in chick embryo (20) and mouse (21), resulting in fewer and smaller metastases *in vivo*. It is also interesting that an inverse relationship between TIMP-1 levels and the rate of cell growth *in vitro* has been demonstrated in both up- and down-regulated cell lines. The TIMP-1 up-regulated cells not only grew more slowly than parental B16F10 cells *in vitro* but also reached a lower saturation density (20, 21). Conversely, down-regulation of TIMP-1 levels in Swiss 3T3 cells led to increased growth rate *in vitro* and a higher saturation density (41). A synthetic matrix metalloproteinase inhibitor reduced the growth of human ovarian carcinoma xenografts in nude mice (32). Transfection of rat embryo cells with the complementary DNA for TIMP-2 reduced the growth rate of these cells after s.c. injection in nude mice (22). In contrast to these reports, addition of human TIMP-1 *in vitro* had a growth-promoting activity on a variety of cell lines (42). These findings suggest that an imbalance of TIMP-1/MMP resulting from overexpression of TIMP-1 may have either inhibitory or growth-promoting activities.

Specific adhesion molecules expressed by tumor cells promote homotypic and heterotypic tumor cell adhesion (43). These interactions are important factors in regulating tumor growth. Different classes of proteases including matrix metalloproteinases can degrade adhesion proteins such as laminin and fibronectin, and fragments of these molecules can induce the expression of proteases by malignant cells (44). We show that overexpression of TIMP-1 can result in an apparent reduction in homotypic contact of cancer cells, possibly due to a reduced degradation of adhesion molecules resulting in altered protease/adhesion feedback.

Several studies have shown that reducing metalloproteinase activity decreases invasive ability *in vitro*; therefore, it has been speculated that reduced extravasation would be the primary *in vivo* consequence of this change. However, the effect of altered TIMP-1/MMP balance on extravasation has never before been examined directly *in vivo*. Our results show that the decreased metastatic ability of TIMP-1 overexpressor cells is due to effects on tumor growth, after cancer cell extravasation has occurred, and not to a decreased ability to extravasate. An understanding of the mechanisms involved in the reduction of tumor growth by TIMP-1 may contribute to the development of new therapeutic approaches, not only against metastasis, but also against untreatable primary tumors.

ACKNOWLEDGMENTS

We thank Dr. Frances P. O'Malley for valuable assistance in the analysis of tissue sections and Sylvia M. Wilson and Mitchell J. Zimmer for excellent technical support.

REFERENCES

1. Fidler, I. J. Tumor heterogeneity and the biology of cancer invasion and metastasis. Cancer Res., *38:* 2651–2660, 1978.
2. Nicolson, G. L. Cancer metastasis—organ colonization and the cell-surface properties of malignant cells. Biochim. Biophys. Acta, *695:* 113–176, 1982.
3. Liotta, L. A. Tumor invasion and metastases: role of the basement membrane. Am. J. Pathol., *117:* 339–348, 1984.
4. Netland, P. A., and Zetter, B. R. Tumor-cell interactions with blood vessels during cancer metastasis. *In:* H. E. Kaiser (ed.), Cancer Growth and Progression—Fundamental Aspects of Cancer, pp. 84–97. Dordrecht, the Netherlands: Kluwer Academic Publishers, 1989.
5. Liotta, L. A. Tumor invasion and metastases: role of the extracellular matrix. Cancer Res., *46:* 1–7, 1986.
6. Liotta, L. A., Tryggvason, K., Garbisa, S., Hart, I., Foltz, C. M., and Shafie, S. Metastatic potential correlates with enzymatic degradation of basement membrane collagen. Nature (Lond.), *284:* 67–68, 1980.
7. Matrisian, L. M. Metalloproteinases and their inhibitors in matrix remodeling. Trends Genet., *6:* 121–125, 1990.
8. Matrisian, L. M. The matrix-degrading metalloproteinases. Bioessays, *14:* 455–463, 1992.
9. Welgus, H. G., Jeffrey, J. J., Eisen, A. Z., Roswit, W. T., and Stricklin, G. P. Human skin fibroblast collagenase: interaction with substrate and inhibitor. Collagen Relat. Res., *5:* 167–179, 1985.
10. Edwards, D. R., Waterhouse, P. Holman, M. L., and Denhardt, D. T. A growth-responsive gene (16C8) in normal mouse fibroblasts homologous to a human collagenase inhibitor with erythroid-potentiating activity: evidence for inducible and constitutive transcripts. Nucleic Acids Res., *14:* 8863–8878, 1986.
11. Stetler-Stevenson, W. G., Krutzsch, H. C., and Liotta, L. A. TIMP-2: identification and characterization of a new member of the metalloproteinase inhibitor family. Matrix, *1* (Suppl.): 299–306, 1992.

12. Pavloff, N., Staskus, P. W., Kishnani, N. S., and Hawkes, S. P. A new inhibitor of metalloproteinases from chicken: ChIMP-3. Athird member of the TIMP family . J. Biol. Chem., *267:* 17321–17326, 1992.
13. Denhardt, D. T., Feng, B., Edwards, D. R., Cocuzzi, E. T., and Malyankar, U. M. Tissue inhibitor of metalloproteinases (TIMP, AKA EPA): structure, control of expression and biological functions. Pharmacol. Ther., *59:* 329–341, 1993.
14. Murphy, G., Reynolds, J. J., and Hembry, R. M. Metalloproteinases and cancer invasion and metastasis. Int. J. Cancer, *44:* 757–760, 1989.
15. Khokha, R., and Denhardt, D. T. Matrix metalloproteinases and tissue inhibitor of metalloproteinases: a review of their role in tumorigenesis and tissue invasion. Invasion Metastasis, *9:* 391–405, 1989.
16. Hicks, N. J., Ward, R. V., and Reynolds, J. J. A fibrosarcoma model derived from mouse embryo cells: growth properties and secretion of collagenase and metalloproteinase inhibitor (TIMP) by tumour cell lines. Int. J. Cancer, *33:* 835–844, 1984.
17. Mignatti, P., Robbins, E., and Rifkin D. B. Tumor invasion through the human amniotic membrane: requirement for a proteinase cascade. Cell, *47:* 487–498, 1986.
18. Khokha, R., Waterhouse, P., Yagel, S., Lala, P. K. Overall, C. M., Norton, G., and Denhardt, D. T. Antisense RNA-induced reduction in murine TIMP levels confers oncogenicity on Swiss 3T3 cells. Science (Washington DC), *243:* 947–950, 1989.
19. Khokha, R, Zimmer, M. J., Graham, C. H., Lala, P. K., and Waterhouse P. Suppression of invasion by inducible expression of tissue inhibitor of metalloproteinase-1 (TIMP-1) in B16-F10 melanoma cells. J. Natl. Cancer Inst., *84:* 1017–1022, 1992.
20. Khokha, R., Zimmer, M. J., Wilson, S. M., and Chambers, A. F. Up-regulation of TIMP-1 expression in B16-F10 melanoma cells suppresses their metastatic ability in chick embryo. Clin. Exp. Metastasis, *10:* 365–370, 1992.
21. Khokha, R., Suppression of the tumorigenic and metastatic abilities of murine B16F10 melanoma cells *in vivo* by the over-expression of the tissue inhibitor of the metalloproteinases-1. J. Natl. Cancer Inst., *86:* 299–304, 1994.
22. DeClerck, Y. A., Perez, N., Shimada, H., Boone, T. C., Langley, K. E., and Taylor, S. M. Inhibition of invasion and metastasis in cells transfected with an inhibitor of metalloproteinases. Cancer Res., *52:* 701–708, 1992.
23. MacDonald, I. C., Schmidt, E. E., Morris, V. L., Chambers, A. F., and Groom, A. C. Intravital videomicroscopy of the chorioallantoic microcirculation: a model system for studying metastasis. Microvasc. Res., *44:* 185–199, 1992.
24. Chambers, A. F., Schmidt, E. E., MacDonald, I. C., Morris, V. L., and Groom, A. C. Early steps in hematogenous metastasis of B16F1 melanoma cells in chick embryos studied by high-resolution intravital videomicroscopy. J. Natl. Cancer Inst., *84:* 797–803, 1992.
25. Morris, V. L., MacDonald, I. C., Koop, S., Schmidt, E. E., Chambers, A. F., and Groom, A. C. Early interactions of cancer cells with the microvasculature in mouse liver and muscle during hematogenous metastasis: videomicroscopic analysis. Clin. Exp. Metastasis, *11:* 377–390, 1993.
26. Fidler, I. J. Biological behavior of malignant cells correlated to their survival *in vivo*. Cancer Res., *35:* 218–224, 1975.
27. Chambers, A. F., Shafir, R., and Ling, V. A model system for studying metastasis using the embryonic chick. Cancer Res., *42:* 4018–4025, 1982.
28. Witte, R. S. Tests for ranked data. *In:* Statistics, Ed. 2, pp.275–292. New York: Holt, Rinehart and Winston, 1985.
29. Ausprunk, D. H., Dethlefsen, S. M., and Higgins, E. R. Distribution of fibronectin, laminin and type IV collagen during development of blood vessels in the chick chorioallantoic membrane. *In:* R. N. Feinberg, G. K. Sherer, and R. Auerbach (eds.), The Development of the Vascular System, pp. 93–108. Basel: Karger, 1991.
30. Fitze-Gschwind, V. Zur Entwicklung der Chorioallantoismembran des Hühnchens. Adv. Anat. Embryol. Cell Biol., *47:* 1–51, 1973.
31. Sethi, N., and Brookes, M. Ultrastructure of the blood vessels in the chick allantois and chorioallantois. J. Anat., *109:* 1–15, 1971.
32. Davies, B., Brown, P. D., East, N., Crimmin, M. J., and Balkwill, F. R. A synthetic matrix metalloproteinase inhibitor decreases tumor burden and prolongs survival of mice bearing human ovarian carcinoma xenografts. Cancer Res., *53:* 2087–2091, 1993.
33. Graf, M., Baici, A., and Sträuli, P. Histochemical localization of cathepsin B at the invasion front of the rabbit V2 carcinoma. Lab. Invest., *45:* 587–596, 1981.
34. Gross, J. L., Moscatelli, D., Jaffe, E. A., and Rifkin, D. B. Plasminogen activator and collagenase production by cultured capillary endothelial cells. J. Cell Biol., *95:* 974–981, 1982.
35. De Bruyn, P. P. H., and Cho, Y. Vascular endothelial invasion via transcellular passage by malignant cells in the primary stage of metastases formation. J. Ultrastruct. Res., *81:* 189–201, 1982.
36. Folkman, J. Endothelial cells and angiogenic growth factors in cancer growth and metastasis. Cancer Metastasis Rev., *9:* 171–174, 1990.
37. Moses, M. A., Sudhalter, J., and Langer, R. Identification of an inhibitor of neovascularization from cartilage. Science (Washington DC), *248:* 1408–1410, 1990.
38. Takigawa, M., Nishida, Y., Suzuki, F., Kishi, J., Yamashita, K., and Hayakawa, T. Induction of angiogenesis in chick yolk-sac membrane by polyamines and its inhibition by tissue inhibitors of metalloproteinases (TIMP and TIMP-2). Biochem. Biophys. Res. Commun., *171:* 1264–1271, 1990.
39. Moses, M. A., and Langer, R. A metalloproteinase inhibitor as an inhibitor of neovascularization. J. Cell. Biochem., *47:* 230–235, 1991.
40. Norton, L. Introduction to clinical aspects of preneoplasia: a mathematical relationship between stromal paracrine autonomy and population size. *In:* P. A. Marks, H. Türler, and R. Weil (eds.), Precancerous Lesions: A Multidisciplinary Approach, Series: Challenges of Modern Medicine, Vol. 1, pp. 269–275. Rome: Ares-Serono Symposia, 1993.
41. Denhardt, D. T., Khokha, R., Yagel, S., Overall, C. M., and Parhar, R. S. Oncogenic consequences of down-modulating TIMP expression in 3T3 cells with antisense RNA. *In:* H. Birkedal-Hansen, Z. Werb, H. G. Welgus, and H. E. Van Wart (eds.), Matrix Supplement No. 1, pp. 281–285. New York: Gustav Fischer Verlag, 1992.
42. Hayakawa, T., Yamashita, K., Tanzawa, K., Uchijima, E., and Iwata, K. Growth-promoting activity of tissue inhibitor of metalloproteinases-1 (TIMP-1) for a wide range of cells. A possible new growth factor in serum. FEBS Lett., *298:* 29–32, 1992.
43. Zetter, B. R. Adhesion molecules in tumor metastasis. Semin. Cancer Biol., *4:* 402.1–402.11, 1993.
44. Werb, Z., Tremble, P. M., Behrendtsen, O., and Crowley, E. Signal transduction through the fibronectin receptor induces collagenase and stromelysin gene expression. J. Cell Biol., *109:* 877–889, 1989.